J. Mol. Biol. (1991) **218**, 685–689

Crystallization and X-ray Diffraction Studies of a Soluble Form of the Human Transferrin Receptor

David W. Borhani† and Stephen C. Harrison‡

Howard Hughes Medical Institute and
Department of Biochemistry and Molecular Biology, Harvard University
7 Divinity Avenue, Cambridge MA 02138, U.S.A.

(Received 28 August 1990; accepted 5 January 1991)

A soluble tryptic fragment of the human transferrin receptor (residues 121 to 760) has been crystallized from 2·8 M-KCl (pH 6·2) and polyethylene glycol 8000. This fragment retains the transferrin-binding activity of intact transferrin receptor. Although the trypsin treatment removes the intermolecular disulfide bonds, the receptor fragment is dimeric both under physiological conditions and at the high salt concentrations used for crystallization. The receptor fragment crystallizes in the orthorhombic space group $P2_12_12_1$, $a = 105{\cdot}5$ Å, $b = 224{\cdot}5$ Å, $c = 363{\cdot}5$ Å. The crystals are extremely radiation sensitive. Their diffraction extends to 3·8 Å, and there is some diffuse scatter with helical characteristics. Analysis of these diffraction patterns indicates that the transferrin receptor fragments are arranged in continuous 8-fold symmetric helical columns parallel to the *c* axis, with a total of 32 receptor fragment monomers in the unit cell. A structure determination is in progress.

Transferrin receptor (TfR§) is a 180,000 M_r integral membrane protein expressed by most mammalian cells (Trowbridge *et al.*, 1984). Transferrin receptor present on the cell surface binds transferrin (Tf), the serum iron transport protein. Endocytosis of the complex leads to release of iron in an acidic compartment. The complex then recycles to the cell surface, where release of apotransferrin leaves the receptor free to begin another cycle of iron uptake (Dautry-Varsat *et al.*, 1983; Klausner *et al.*, 1983*a*,*b*). TfR mediates the bulk of specific, saturable iron uptake by cells. Its presence on cell surfaces is therefore essential for cellular survival and growth, especially in rapidly dividing cells (Sutherland *et al.*, 1981; Trowbridge & Omary, 1981). Both TfR itself (Schneider *et al.*, 1982) and the expression of its gene have been extensively characterized (McClelland *et al.*, 1984; Klausner & Harford, 1989). There has been interest in using the transferrin–transferrin receptor pathway to ferry foreign molecules (e.g. DNA or drugs) into cells (Wagner *et al.*, 1990).

† Present address: BioCryst, Inc., 1075 13th Street South, Suite 310, Birmingham AL 35205, U.S.A.

‡ Author to whom all correspondence should be addressed.

§ Abbreviations used: TfR, transferrin receptor; Tf, transferrin; TfR-t, transferrin receptor extracellular fragment; PEG, polyethylene glycol.

Human TfR was purified from term placentae. Our purification yields the intact protein, a disulfide-linked dimer of total M_r 180,000, solubilized in detergents (Turkewitz *et al.*, 1988*a*). Digestion with trypsin generates a large extracellular fragment, which we refer to as TfR-t. TfR-t has Arg121 at its amino terminus (Turkewitz *et al.*, 1988*a*). It has therefore lost the N-terminal intracellular portion of the receptor, the hydrophobic membrane-spanning anchor, and an additional 30 extracellular amino acid residues, including the two cysteine residues that form intramolecular disulfide bonds (Jing & Trowbridge, 1987). Under denaturing gel electrophoresis in the presence or absence of reducing agents, TfR-t migrates as a monomer of M_r 70,000. However, both non-denaturing gel electrophoresis and gel filtration (Superose 6, Pharmacia-LKB Biotechnology, Inc., Piscataway, NJ) indicate that TfR-t has an M_r of 140,000, as expected for a dimer. Isoelectric focusing of TfR-t under native conditions shows that it is composed of at least six species, whose isoelectric points range from 5·7 to 6·5. Neuraminidase digestion of TfR-t substantially decreases, but does not eliminate, the heterogeneity, while raising the average pI to 7·5. In the presence of two equivalents of iron-saturated Tf, TfR-t forms a complex of M_r 300,000, an $\alpha_2\beta_2$ tetramer. We have crystallized both TfR-t and its complex with Tf.

0022-2836/91/080685-05 $03.00/0

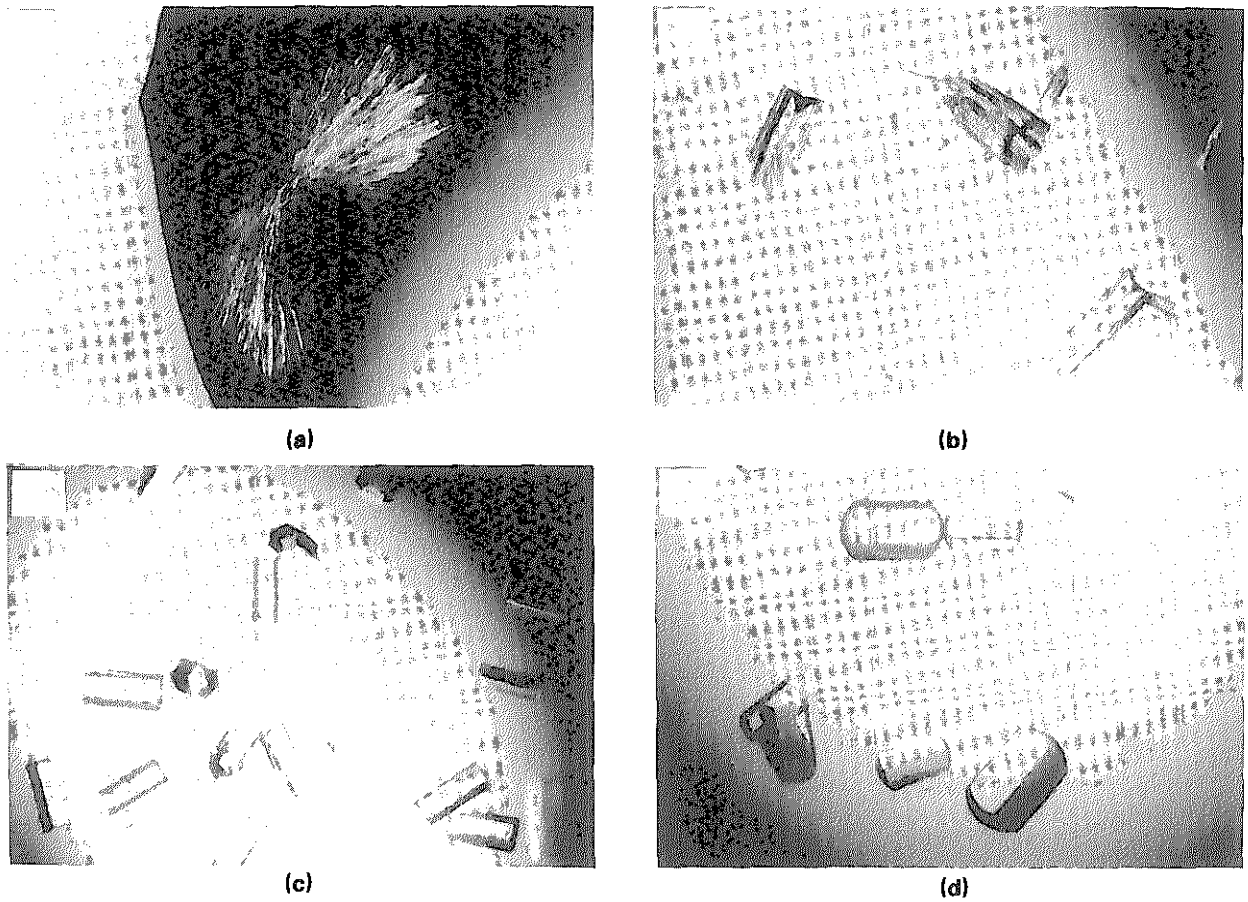

Figure 1. Crystals of the extracellular fragment of the human transferrin receptor TfR-t. The effect of increasing salt concentration on the crystal morphology is shown. TfR-t (5 mg/ml in 150 mM-NaCl, 25 mM-Hepes, pH 7·5) was crystallized by mixing equal volumes of the protein and precipitant solutions; the hanging drop was then equilibrated with a reservoir of the precipitant solution. Crystals were grown at 20 °C in: (a) 1·2 M-KCl, 9·9% PEG 8000, 100 mM-Pipes (pH 6·5); (b) 2·0 M-KCl, 6·1% PEG 8000, 50 mM-Pipes (pH 6·3); (c) 2·4 M-KCl, 6·1% PEG 8000, 100 mM-Pipes (pH 6·3); (d) 2·8 M-KCl, 100 mM-$MgCl_2$, 3·0% PEG 8000, 50 mM-Pipes (pH 6·3). The prominent faces are {1 1 0}, with the *a* axis extending up between these 2 faces. The {0 1 0} faces are developed to a smaller extent.

We have obtained very small clusters of needle-like crystals from the purified complex of Fe_2Tf and TfR-t. The needles grow from 100 mM-Tris (pH 7·7 to 9·0), 5% to 10% (v/v) glycerol, 3% to 8% (w/v) polyethylene glycol (PEG) 20,000, [Fe_2Tf·TfR-t] 10 to 15 mg/ml at room temperature by vapor diffusion in hanging drops. Gel electrophoresis of carefully washed, redissolved needles indicated that these crystals contain equimolar amounts of Tf and TfR-t. Attempts to increase the size of these crystals have so far been unsuccessful.

TfR-t crystallizes from mixtures of a variety of salts and PEGs of different molecular weights. Needle-like crystals were obtained from 0·5 to 1·0 M-KCl, 8% to 10% PEG 8000, 50 to 100 mM-Pipes (pH 6·5) at room temperature. These needles were very narrow, but their size could be increased to about 250 μm × 50 μm × 10 μm by seeding. Modification of crystallization conditions led to larger and better-ordered crystals, which grow at temperatures from 18 to 30 °C in the presence of NaCl, KCl or $(NH_4)_2SO_4$ and PEG 3000, 8000 or 20,000 at pH 6·0 to 7·0. Crystals are not obtained below pH 6, presumably due to aggregation of TfR-t (Turkewitz *et al.*, 1988*b*). Ionic strength is a critical variable (see Fig. 1). At low ionic strength, TfR-t crystallizes as needles. Increasing the KCl concentration from 1·2 M to 2·0 M leads to a coalescence of the needles, and a further increase to 2·4 or 2·8 M yields well-formed tablets, which show sharp extinctions between crossed polarizers. As the concentration of KCl increases, the concentration of PEG required to produce crystals drops; crystals can be grown from 3·0 M-KCl in the absence of PEG. The divalent cations Mg^{2+} and Ca^{2+} have little effect on the crystallization. Our best crystals are obtained from 2·8 M-KCl, 25 mM-KPO_4 (pH 6·2 to 6·8), 3% to 6% PEG 8000, [TfR-t] 5 to 15 mg/ml in hanging drops at 20 °C. They grow to a maximum size of 350 μm × 250 μm × 150 μm in one to two weeks.

Since TfR-t is a non-covalent dimer, it was of interest to determine its state of aggregation under the high salt conditions used to obtain crystals. Gel filtration of TfR-t at 2·8 M-KCl, 20 mM-KPO_4 (pH 6·5, Superose 6) showed that TfR-t migrates

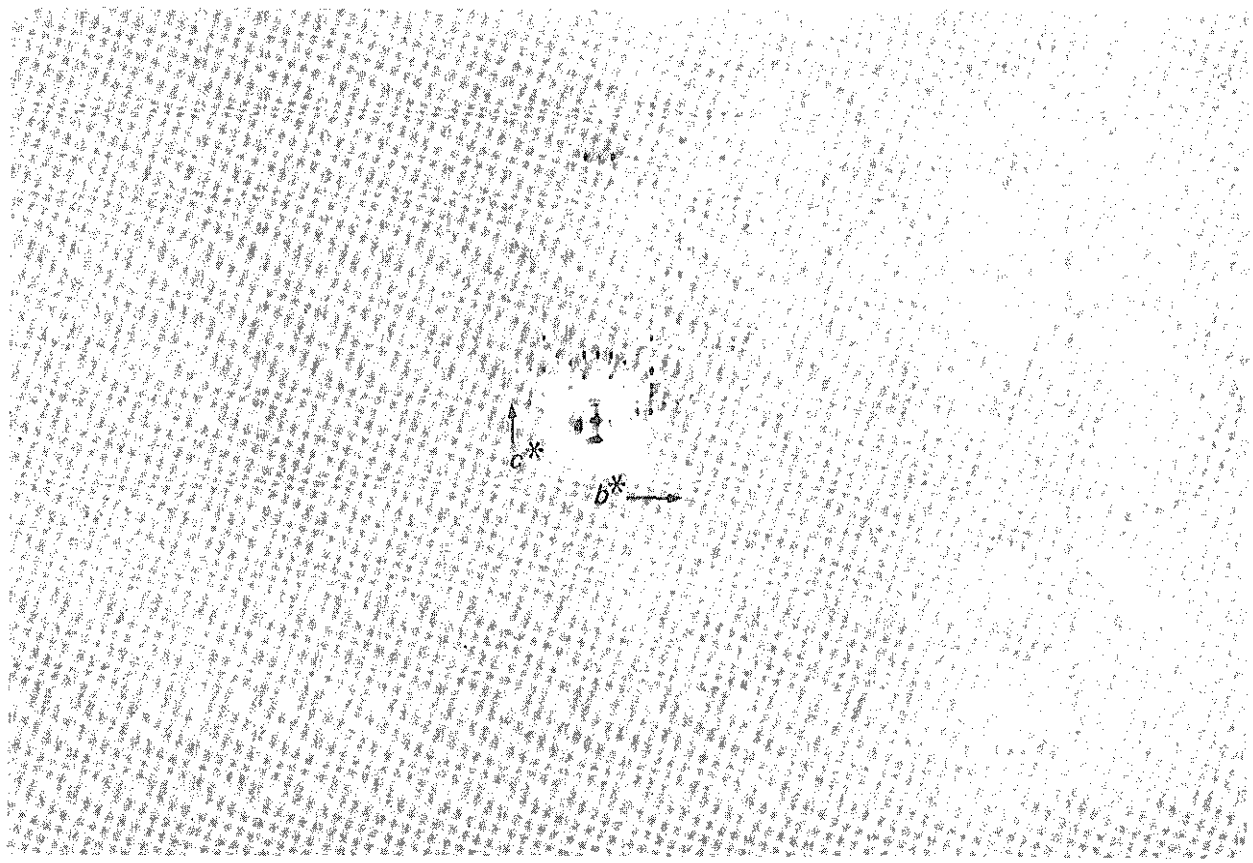

Figure 2. Oscillation photograph of a TfR-t crystal showing the non-crystallographic 8-fold screw axis along c^*. In this 5° oscillation photograph, aligned with a^* along the X-ray beam, b^* is horizontal and c^* is vertical. In the [0 k l] layer, note especially the absence of 0 0 l reflections when $l \neq 8n$. Especially prominent are reflections 0, 0, 32; 0, ±1, 32; 0, 0, 40; and 0, ±1, 40. These correspond to helical diffraction layer-lines.

with an apparent M_r of 140,000, i.e. as a dimer. Under the same conditions, Fe_2Tf elutes as a monomer, apparent M_r 80,000. Denaturing polyacrylamide gel electrophoresis of the crystals indicates that they are composed of the 70,000 M_r fragment of the transferrin receptor. Isoelectric focusing of the TfR-t crystals reveals a distribution of isoforms similar to that seen with uncrystallized TfR-t. Neuraminidase digestion of TfR-t has no effect on its crystallization.

The space group of the TfR-t crystals is $P2_12_12_1$, $a = 105{\cdot}5$ Å, $b = 224{\cdot}5$ Å, $c = 363{\cdot}5$ Å (1 Å = 0·1 nm). The diffraction pattern extends to 3·8 Å, but there is a significant drop in the intensity of the molecular transform at 7 Å resolution. The crystals are extremely radiation sensitive; the typical lifetime on a GX-13 rotating anode generator (2·4 kW) is two hours. Radical-trapping agents or cooling do not decrease this sensitivity. Neuraminidase-treated TfR-t crystallizes in the same unit cell as the untreated material; these crystals diffract as well as the TfR-t crystals, and they are as radiation sensitive.

Several unusual properties of the TfR-t crystals have enabled us to devise a packing model for the TfR-t molecules in the $P2_12_12_1$ unit cell. We observe only those reflections 0 0 l, $l = 8n$ on the long c axis of the crystals (see Fig. 2). This observation indicates that there is a non-crystallographic 8-fold screw axis parallel to the c axis of the unit cell, and we infer that the TfR-t dimers are arranged in 8-fold symmetric helical columns lying along the c axis. This interpretation is supported by the following observations. (1) Off-lattice diffuse scatter characteristic of a helical diffraction pattern is observed on most oscillation photographs of the TfR-t crystals that have c^* near the surface of the Ewald sphere. (2) Radiation-damaged crystals usually break into fibrils parallel to the c axis. (3) Crystallization of TfR-t under low salt conditions affords needles elongated along the c axis.

In the $P2_12_12_1$ unit cell, crystallographic 2_1 screw axes parallel to z are located at $(x, y) = (1/4, 0)$, $(3/4, 0)$, $(1/4, 1/2)$ and $(3/4, 1/2)$. The non-crystallographic 8-fold screw axis must be coincident with a crystallographic screw axis. The TfR-t helices are centered at $(1/4, 0)$ and $(3/4, 1/2)$, with one helix running along $+z$ and the other running along $-z$, leading to nearly hexagonal close-packing of the helices in the (x, y) plane (see Fig. 3). This packing model requires that there be four TfR-t dimers in an asymmetric unit, and thus 32 TfR-t monomers in the unit cell. Each unit cell contains approximately 2,250,000 daltons of protein; the solvent content is about 68%.

Oscillation photographs of the highly mosaic,

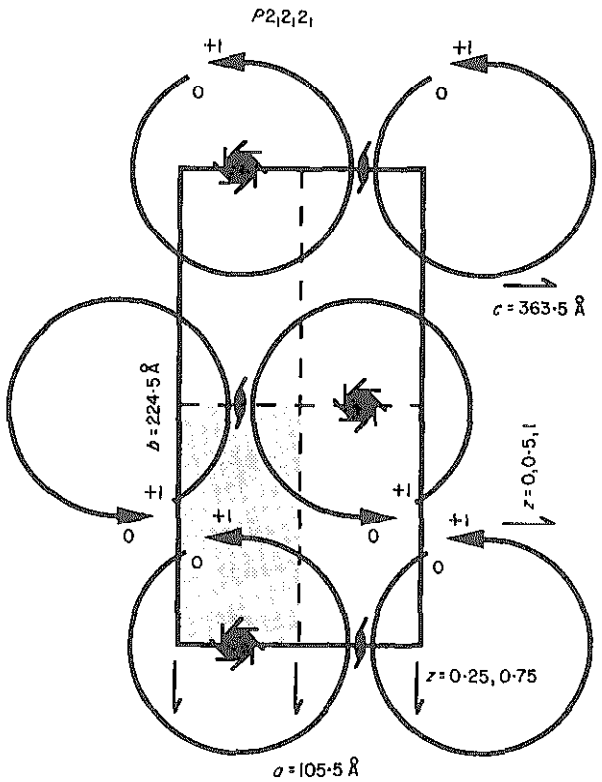

Figure 3. Packing model for the helical columns of TfR-t in the $P2_12_12_1$ unit cell. One unit cell is shown in projection down the c axis. Broken lines delineate asymmetric unit boundaries. Each TfR-t column is represented by a curved arrow. The z values given at the beginning and end of each arrow are meant to illustrate the direction of the helical stacking; the 2 helical columns in the unit cell run in opposite directions along the z axis. Columns are centered at $(x, y) = (1/4, 0)$ and $(3/4, 1/2)$. Both the crystallographic and non-crystallographic symmetry axes are shown.

needle-like crystals of TfR-t grown at low ionic strength show a 53 Å spacing perpendicular to the needle axis and a 1078 Å spacing parallel to the needle axis; systematic absences along this axis suggest that the crystals have approximate 24-fold screw-axis symmetry in this direction. The packing in these crystals can be related to the high-salt crystal packing model in the following manner. We assume that the TfR-t helices, with a diameter approximately equal to the smallest unit cell dimension (105·5 Å), are aligned along the helix axis with rotational disorder. Then perpendicular to the helix axis one would see X-ray diffraction, as observed, at a spacing equal to the helix radius (53 Å), i.e. $a/2$ in the $P2_12_12_1$ cell. Furthermore, if the 8-fold symmetry in the TfR-t crystals were distorted such that the true helical repeat occurred only every three turns, then the unit cell would be $3 \times 363{\cdot}5 = 1090{\cdot}5$ Å long, very close to that seen in the low salt crystals. In addition only every 24th reflection would be observed along the helix axis.

There are four possible 8-fold screw axes that are consistent with the high-salt packing model; 8_1, 8_3, 8_5 and 8_7. In an 8_1 helix, the helical subunits are related by a right-handed rotation of 45° about the helix axis, and a translation along this axis of $1/8$ z (helical repeat distance). In an 8_3 helix, the rotation is 135°. An 8_5 helix is a left-handed 8_3 helix, and the 8_7 and 8_1 helices are similarly related. In the diffuse scatter, we observe strong meridional layer-lines centered on reflections 0, 0, 32 and 0, 0, 40. Off-meridional layer-lines are centered on 0, ±8, 37; 0, ±11, 37; 0, ±4, 38; 0, ±10, 40; and 0, ±7, 43. The helical selection rules differ for 8_1 and 8_3 helices, and thus different Bessel terms contribute to the layer-lines in each case. Analysis of the positions of the observed layer-lines suggests that the TfR-t dimers are arranged in an 8_1 (or 8_7) helix with mean radius of 25 Å or in an 8_3 (or 8_5) helix with mean radius of 35 Å. We observe diffuse helical diffraction only at about 10 Å resolution, implying a strong 10 Å repeat along the helix axis. This observation suggests that α-helical bundles, directed perpendicular to the major (8-fold) screw axis, may form part of the TfR-t structure.

We have collected oscillation film data from native TfR-t crystals and $SmCl_3$-derivative crystals at various synchrotron radiation sources, and efforts toward a structure determination are in progress.

We thank Marina Babyonyshev for excellent technical assistance, and David Rodgers, Barbara Harris and Robert Liddington for helpful discussions. We are grateful to Dr M. Epstein (Peter Bent Brigham Hospital) for assistance in obtaining placentae. We thank the staff of the protein crystallography group of SERC Daresbury Laboratory for assistance and the SERC for beam time. Part of the support for this work came from NIH grant CA-13202 (to S.C.H.).

References

Dautry-Varsat, A., Ciechanover, A. & Lodish, H. F. (1983). pH and the recycling of transferrin during receptor-mediated endocytosis. *Proc. Nat. Acad. Sci., U.S.A.* **80**, 2258–2262.

Jing, S. & Trowbridge, I. S. (1987). Identification of the intermolecular disulfide bonds of the human transferrin receptor and its lipid-attachment site. *EMBO J.* **6**, 327–331.

Klausner, R. D. & Harford, J. B. (1989). Cis-trans models for post-transcriptional gene regulation. *Science*, **246**, 870–872.

Klausner, R. D., Van Renswoude, J., Ashwell, G., Kempf, C., Schechter, A. N., Dean, A. & Bridges, K. R. (1983*a*). Receptor-mediated endocytosis of transferrin in K562 cells. *J. Biol. Chem.* **258**, 4715–4724.

Klausner, R. D., Ashwell, G., Van Renswoude, J., Harford, J. B. & Bridges, K. R. (1983*b*). Binding of apotransferrin to K562 cells: explanation of the transferrin cycle. *Proc. Nat. Acad. Sci., U.S.A.* **80**, 2263–2266.

McClelland, A., Kuhn, L. C. & Ruddle, F. H. (1984). The human transferrin receptor gene: genomic organization, and the complete primary structure of the receptor deduced from a cDNA sequence. *Cell*, **39**, 267–274.

Schneider, C., Sutherland, R., Newman, R. & Greaves, M. (1982). Structural features of the cell surface receptor

for transferrin that is recognized by the monoclonal antibody OKT9. *J. Biol. Chem.* **257**, 8516–8522.

Sutherland, R., Delia, D., Schneider, C., Newman, R., Kemshead, J. & Greaves, M. (1981). Ubiquitous cell-surface glycoprotein on tumor cells is proliferation-associated receptor for transferrin. *Proc. Nat. Acad. Sci. U.S.A.* **78**, 4515–4519.

Trowbridge, I. S. & Omary, M. B. (1981). Human cell surface glycoprotein related to cell proliferation is the receptor for transferrin. *Proc. Nat. Acad. Sci., U.S.A.* **78**, 3039–3043.

Trowbridge, I. S., Newman, R. A., Domingo, D. L. & Sauvage, C. (1984). Transferrin receptors: structure and function. *Biochem. Pharmacol.* **33**, 925–932.

Turkewitz, A. P., Amatruda, J. F., Borhani, D., Harrison, S. C. & Schwartz, A. L. (1988*a*). A high yield purification of the human transferrin receptor and properties of its major extracellular fragment. *J. Biol. Chem.* **263**, 8318–8325.

Turkewitz, A. P., Schwartz, A. L. & Harrison, S. C. (1988*b*). A pH-dependent reversible conformational transition of the human transferrin receptor leads to self-association. *J. Biol. Chem.* **263**, 16309–16315.

Wagner, E., Zenke, M., Cotten, M., Beug, H., Birnstiel, M. L. (1990). Transferrin-polycation conjugates as carriers for DNA uptake into cells. *Proc. Nat. Acad. Sci., U.S.A.* **87**, 3410–3414.

Edited by A. Klug